

Springer Series in Optical Sciences 199

Oleksiy Shulika
Igor Sukhoivanov *Editors*

Contemporary Optoelectronics

Materials, Metamaterials and Device
Applications

 Springer

Editors

Oleksiy Shulika
Departamento de Ingeniería Electrónica,
Campus Irapuato-Salamanca
Universidad de Guanajuato
Salamanca
México

Igor Sukhoivanov
Departamento de Ingeniería Electrónica,
Campus Irapuato-Salamanca
Universidad de Guanajuato
Salamanca
México

ISSN 0342-4111

ISSN 1556-1534 (electronic)

Springer Series in Optical Sciences

ISBN 978-94-017-7314-0

ISBN 978-94-017-7315-7 (eBook)

DOI 10.1007/978-94-017-7315-7

Library of Congress Control Number: 2015945602

Springer Dordrecht Heidelberg New York London

© Springer Science+Business Media Dordrecht 2016

This work is subject to copyright. All rights are reserved by the Publisher, whether the whole or part of the material is concerned, specifically the rights of translation, reprinting, reuse of illustrations, recitation, broadcasting, reproduction on microfilms or in any other physical way, and transmission or information storage and retrieval, electronic adaptation, computer software, or by similar or dissimilar methodology now known or hereafter developed.

The use of general descriptive names, registered names, trademarks, service marks, etc. in this publication does not imply, even in the absence of a specific statement, that such names are exempt from the relevant protective laws and regulations and therefore free for general use.

The publisher, the authors and the editors are safe to assume that the advice and information in this book are believed to be true and accurate at the date of publication. Neither the publisher nor the authors or the editors give a warranty, express or implied, with respect to the material contained herein or for any errors or omissions that may have been made.

Printed on acid-free paper

Springer Science+Business Media B.V. Dordrecht is part of Springer Science+Business Media
(www.springer.com)

7	Gyrotropic Metamaterials and Polarization Experiment in the Millimeter Waveband	115
	S.I. Tarapov, S. Yu Polevov and N.N. Beletski	
8	Dynamic Singular Vector Speckle Fields and Their Hurst Exponent Time Analysis	131
	Marat Soskin and Vasyil Vasil'ev	
 Part III Devices of Contemporary Optoelectronics		
9	Synthetic Structures with Parity-Time Symmetry	147
	Tsampikos Kottos and Alejandro B. Aceves	
10	Nonlinear Plasmonic Waveguides	163
	José Ramón Salgueiro and Yuri S. Kivshar	
11	Oppositely Directional Coupler: Example of the Forward Backward Waves Interaction in the Metamaterials.	181
	A.I. Maimistov and E.V. Kazantseva	
12	Characterization of Photonic Crystal Fibers: Selected Methods and Experience	197
	Krzysztof Borzycki and Kay Schuster	
13	All-Normal-Dispersion Photonic Crystal Fibers Under Prism of Supercontinuum Generation and Pulse Compression	219
	Igor A. Sukhoivanov, Sergii O. Iakushev, Oleksiy V. Shulika, Antonio Diez, Miguel V. Andrés, Igor V. Guryev, José Amparo Andrade Lucio and Oscar G. Ibarra Manzano	
	Index	233

Chapter 7

Gyrotropic Metamaterials and Polarization Experiment in the Millimeter Waveband

S.I. Tarapov, S. Yu Polevoy and N.N. Beletski

Abstract The paper deals with the analysis of modern situation in physics of artificial gyrotropic media. Most widespread techniques of experimental and theoretical finding constitutive parameters are under analysis. Besides, the original results obtained by authors while studying polarization features for some types of magnetically controllable metamaterials, possessing the gyrotropic/chiral features in the millimeter wavelength range are presented. The results of measurements are under discussion.

7.1 Introduction

It is well known that the term “gyrotropy”, which was used for description of condensed media dozens years ago, can be applied successfully to the electrodynamics of artificial media (metamaterials). Moreover, a lot of terms, which describe the ability of medium to rotate the polarization of linearly polarized wave (“chirality”, “magnetoactivity”, “bianisotropy”) came from the condensed media physics. They are used widely in physics of metamaterials today. Let consider them more detailed.

In most general case the constitutive parameters ($\hat{\epsilon}$ and $\hat{\mu}$) for the bianisotropic medium [1, 2], represent themselves matrixes, where all components are not equal to zero. The gyrotropic medium as the special case of bianisotropic medium, has anti-symmetric tensor parameters $\hat{\epsilon}$ and $\hat{\mu}$ [3] with non-zero nondiagonal components ($a_{12} = -a_{21} \neq 0$). If the gyrotropic medium has nondiagonal components $a_{12}(\vec{k}) = a_{12}(-\vec{k})$, $a_{21}(\vec{k}) = a_{21}(-\vec{k})$, where \vec{k} is the propagation constant of the media, it is a non-reciprocal medium. Note this medium is represented in our paper by magnetoactive media. The chiral medium, as another special case of gyrotropic medium is a reciprocal medium [4, 5] with nondiagonal components

S.I. Tarapov (✉) · S.Y. Polevoy · N.N. Beletski
O. Ya Usikov Institute for Radiophysics and Electronics of NAS of Ukraine,
Kharkiv, Ukraine
e-mail: tarapov@ire.kharkov.ua

$a_{12}(\vec{k}) = -a_{12}(-\vec{k})$, $a_{21}(\vec{k}) = -a_{21}(-\vec{k})$. Note that the wave propagation in the gyrotropic media for the condensed media were studied in details (for example, [6, 7]), namely for the physics of crystals for the optical frequency band.

The paper presented should be considered as a next step in experimental research of artificial gyrotropic media with electrical and magnetic activity in microwave band. Namely main objectives of study are:

- the development of the experimental technique for determining the effective constitutive parameters of chiral media in the millimeter waveband;
- learning the possibility of experimental control of the rotation angle of the polarization plane of electromagnetic wave by changing the “specific density” of the structure;
- to study both theoretically and experimentally the polarization properties of one-layered and multilayered magnetoactive metamaterial depending on static magnetic field;
- the experimental and numerical demonstration of the Faraday effect enhancement for the case of gyrotropic magnetic layer inserted into special one-dimensional (1D) photonic crystal.

The task of research of chiral metamaterials is interesting both for fundamental and for applied physics. These structures can be used for design the compact magnetically controllable microwave devices, (for inst. polarizers, using the Faraday effect).

Bulk chiral metamaterials are promising, because they can realize rotation of polarization plane of the electromagnetic waves on large angles in the millimeter wavelength range. For example, in [8, 9], the chiral metamaterials used for the rotation of the polarization plane at angles up to several hundred degrees per wavelength, which is several orders of magnitude larger than for the natural media with optical activity. In spite a lot of studies are carrying out now (for example [10, 11]), a plenty of tasks for the millimeter waveband which is important today from the application point of view, are unsolved yet.

Probably, Hetch and Barron [12], Arnaut and Davis [13] were the first who introduced planar (2D) chiral structures into the electromagnetic research. However, 2D chirality does not lead to the same electromagnetic effects which are conventional for 3D chirality so, it became a subject of special intense investigations [14]. It is known, that bulk (3D) chiral artificial structures [1] manifest a reciprocal optical activity [15]. The typical constructive object of 3D chiral media is a spirally conducting cylinder. Besides, in some particular cases, quasi-2D planar chiral metallic structures can be asymmetrically combined with isotropic substrates to distinguish a reciprocal optical response inherent to true 3D chiral structures. In such metamaterials, at normal incidence of the exciting wave, an optical activity appears only in the case, when their constituent metallic elements have finite thickness, which provides an asymmetric coupling of the fields at the air and substrate interfaces.

The planar chiral structure placed on a ferrite substrate [10, 15] (one layered magnetoactive structure) and multilayered ferrite-dielectric structures [16] are even more interesting objects from both fundamental and application points of view. The

appearance of so-called Faraday Effect Enhancement (FEE) has significant application perspectives. Namely, they can be used successfully to design non-reciprocal magnetically controllable microwave devices based on the Faraday effect.

A number of principal features of gyrotropy of magnetoactive medium can be extracted while studying the bounded photonic crystal (PC) [17]. In particular, we note the appearance of a sharp transparency peak (Tamm peak) in the band gap of such a structure. This effect is based on the well-known Tamm state effect [18, 19]. This phenomenon is well studied experimentally for magnetoactive one-dimensional and two-dimensional periodical media [20–23] (in non-gyrotropic approximation). But the presence of gyrotropy in such medium is of special interest. The wave propagation in the photonic crystal substantially depends on the material which includes into PC, and on the material placed as a boundary of the PC. For the gyrotropic boundary medium we can obtain the Faraday Effect Enhancement (FEE) [17] also. It reveals here as a strong rotation of the polarization plane by such PC on the frequency of Tamm state. A significant Faraday Effect Enhancement (FEE) in the case when magneto-optical PC, bounded by almost reflecting medium was described theoretically in [16]. The FEE for microwave band was observed for bounded PC, which is formed by magnetoactive elements [17]. So the FEE effect can be considered as a resonance effect in gyrotropic resonator without intrinsic volume.

Note that in contrast to optical frequency range photonic crystals, in the microwave band we are dealing with magnetic gyrotropy instead electric gyrotropy. One of the most actual directions of the photonic and magnetophotonic crystals study is searching ways to control the spectral properties of such structures in the microwave frequency range. It allows to produce a novel generations of high-speed electronically controlled devices that may find wide application in the area of telecommunications, computing and physical electronics.

7.2 The Polarization Rotation Enhancement in the Dielectric Bulk Chiral Metamaterial

7.2.1 The Experimental Setup

The experimental setup for the determination of effective constitutive parameters of chiral media is shown on Fig. 7.1 [24]. Investigated bulk chiral structure is placed between the transmitting and receiving rectangular horns which are fitted to the Vector Network Analyzer Agilent N5230A by means of coaxial-waveguide junctions and cables. The main functions of the Analyzer are measuring S-parameters, its processing and transforming into the graphical form. Absorbing screen can be placed in the vicinity of the structure under study to eliminate the influence of diffraction on the edges.

The horns are located on the same axis passing perpendicularly to the structure through its center at a distance larger than ten wavelengths. If necessary, the phase-correction lenses can be placed close the horns that make the wavefront flat.

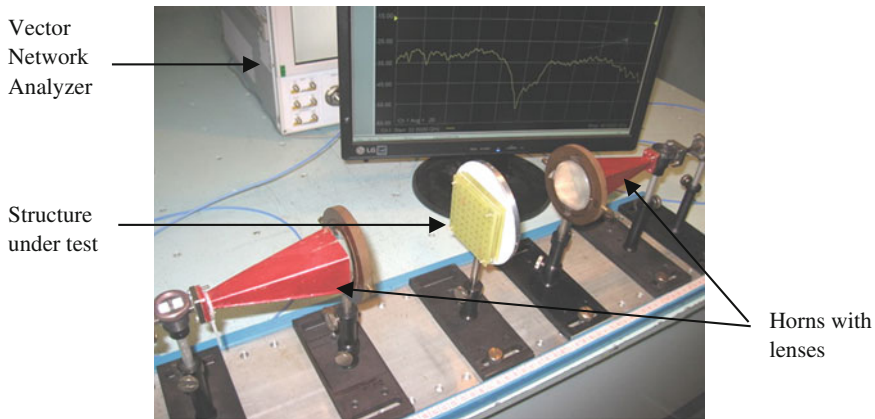
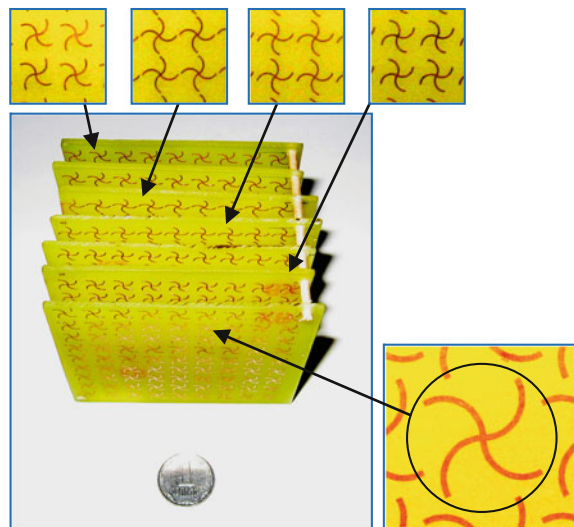


Fig. 7.1 The experimental setup for study of gyrotropic/chiral metamaterials

Receiving horn can be rotated around its axis. With help of the analyzer the parameters S_{21} and S_{11} in the frequency range of 22–40 GHz are registered. The calibrating procedure for the measuring setup provides the reduction in the influence of parasitic reflections occurred due to the non-ideality matching of the spatial elements.

The determination of the chirality parameter was carried out using the model bulk dielectric chiral structure (Fig. 7.2). It consists of several subsequent layers of planar chiral structures in the form of 2D array of chiral elements on the fiberglass substrate. Planar chiral structures were etched on the foil side of the fiberglass by

Fig. 7.2 Model dielectric bulk chiral structure under study



photolithography. Chiral elements are rotated around its axis by 15° relative to the elements in each subsequent layer.

7.2.2 Determination of the Effective Constitutive Parameters of Chiral Media

To obtain the comprehensive information about the gyrotropic medium it is necessary to have technique of mathematical description of its constitutive parameters. Since there are several forms of writing the constitutive equations for chiral media, so first we must select a convenient form of the constitutive equations, such as [4, 25]:

$$\vec{D} = \hat{\epsilon}\vec{E} + i\hat{\kappa}\vec{H}, \quad \vec{B} = \hat{\mu}\vec{H} - i\hat{\kappa}\vec{E}, \quad (7.1)$$

where \vec{E} , \vec{H} are vectors of the electric and magnetic fields intensity; \vec{D} , \vec{B} are vectors of electric and magnetic induction, $\hat{\epsilon}$, $\hat{\mu}$ are the complex permittivity and permeability; $\hat{\kappa}$ is the complex chirality parameter.

To make the problem clearer let's consider the task about the propagation of the electromagnetic wave through the chiral layer of finite thickness L . Let's consider the case of normal incidence of the plane electromagnetic waves. In this case, the chiral medium is a uniaxial medium in the direction of wave propagation (z axis).

Using the transfer matrix method, we can obtain the relations between the components of the electric and magnetic fields intensities (E_x , E_y , H_x , H_y) on the input and output boundary of the chiral layer ($z = 0$ and $z = L$) and its constitutive parameters ($\hat{\epsilon}$, $\hat{\mu}$, $\hat{\kappa}$):

$$\Psi(L) = \hat{M}\Psi(0), \quad (7.2)$$

$$\Psi(L) = \begin{pmatrix} E_x(L) \\ E_y(L) \\ H_x(L) \\ H_y(L) \end{pmatrix}, \quad \Psi(0) = \begin{pmatrix} E_x(0) \\ E_y(0) \\ H_x(0) \\ H_y(0) \end{pmatrix},$$

where \hat{M} is the transfer matrix 4×4 with coefficients:

$$M_{11} = M_{22} = M_{33} = M_{44} = \cos(\hat{\kappa}L) \cos(k_0\hat{\kappa}L),$$

$$M_{12} = -M_{21} = M_{43} = -M_{34} = \cos(\hat{\kappa}L) \sin(k_0\hat{\kappa}L),$$

$$M_{13} = M_{24} = -i\frac{\hat{\mu}}{\hat{n}} \sin(\hat{\kappa}L) \sin(k_0\hat{\kappa}L),$$

$$M_{14} = -M_{23} = i\frac{\hat{\mu}}{\hat{n}} \sin(\hat{\kappa}L) \cos(k_0\hat{\kappa}L),$$

$$M_{31} = M_{42} = i \frac{\dot{n}}{\dot{\mu}} \sin(\dot{k}L) \sin(k_0 \dot{\kappa}L),$$

$$M_{41} = -M_{32} = i \frac{\dot{n}}{\dot{\mu}} \sin(\dot{k}L) \cos(k_0 \dot{\kappa}L),$$

where $\dot{k} = k_0 \dot{n}$, $\dot{n} = \sqrt{\dot{\epsilon} \dot{\mu}}$, and k_0 is the propagation constant of the vacuum.

Thus, using the relation (7.2) and setting the constitutive parameters, we can find the transmission coefficients for the electric and magnetic fields intensity, and polarization characteristics of chiral layer.

However, an inverse problem of determining the effective constitutive parameters of such media using experimentally measured transmission and reflection coefficients exists as well. It appears to be even more important from the experimental point of view. There are several approaches of experimental determination of the effective constitutive parameters of uniaxial chiral media [5, 25].

The *first approach* described in [9, 25], consists of measuring the transmission and reflection coefficients of electromagnetic waves interacting with the metamaterial for two mutual orientations of transmitting and receiving horns. This means—the “parallel” (co-polarization) and “perpendicular” (cross-polarization) horns locations. Measured transmission and reflection coefficients for co-polarization (\dot{T}_{\parallel} , \dot{R}_{\parallel}), and for cross-polarization (\dot{T}_{\perp} , \dot{R}_{\perp}) are associated with the transmission and reflection coefficients of electromagnetic waves with right (RCP) and left (LCP) circular polarizations [9]:

$$\dot{T}_{\pm} = \dot{T}_{\parallel} \mp i \dot{T}_{\perp}, \quad \dot{R}_{\pm} = \dot{R}_{\parallel} = \dot{R}. \quad (7.3)$$

Calculating the values of \dot{T}_{+} and \dot{T}_{-} allows to calculate the chirality parameter $\dot{\kappa}$ and polarization characteristics: the rotation angle of the polarization plane of the transmitted wave θ and the ellipticity angle η [25].

Permittivity $\dot{\epsilon}$, permeability $\dot{\mu}$ and chirality parameter $\dot{\kappa}$ for the chiral medium are determined by the following relations [25]:

$$\dot{\epsilon} = \dot{n}/\dot{Z}, \quad \dot{\mu} = \dot{n}\dot{Z}, \quad \dot{\kappa} = (\dot{n}_{+} - \dot{n}_{-})/2, \quad (7.4)$$

where $\dot{n} = (\dot{n}_{+} + \dot{n}_{-})/2 = \sqrt{\dot{\epsilon} \dot{\mu}}$ is the average refractive index for RCP and LCP waves. The refraction coefficients \dot{n}_{+} , \dot{n}_{-} of the RCP and LCP waves and impedance \dot{Z} are determined from transmission \dot{T}_{\pm} and reflection \dot{R}_{\pm} coefficients [25].

Thus, by measuring the transmission and reflection coefficients for the waves on co-polarization and cross-polarization with the horns, we can calculate the effective constitutive parameters of the structure, and its polarization characteristics.

There is also a *second approach* of determining the chirality parameter $\dot{\kappa}$ and the polarization characteristics of the transmitted wave for the chiral structure. It suggests the direct measurement of the angle θ using the receiving horn, which can be rotated around its longitudinal axis [5]. The angle θ is that rotation angle of the

receiving horn at which the transmission coefficient of electromagnetic waves is maximal (\dot{T}_{\max}). If we measure the minimum transmission coefficient (\dot{T}_{\min}) at a rotation angle of the receiving horn $\theta + 90^\circ$, then we can determine the ellipticity angle η of the transmitted wave by the following relation:

$$\eta = \arctg \frac{|\dot{T}_{\min}|}{|\dot{T}_{\max}|}. \quad (7.5)$$

Let us find the relation between the polarization characteristics of the structure and its chirality parameter. The rotation angle of the polarization plane is directly proportional to the angular frequency ω , the real part of the chirality parameter and the chiral layer thickness [4, 26]:

$$\theta = k_0 L \kappa' = \frac{\omega L \kappa'}{c}. \quad (7.6)$$

The ellipticity angle of the transmitted wave depends on the imaginary part of the chirality parameter [27] as:

$$\eta = \arctg[\text{th}(k_0 L \kappa'')]. \quad (7.7)$$

Finally according to the experimental values θ and η one can calculate the chirality parameter:

$$\dot{\kappa} = \frac{\theta}{k_0 L} + i \frac{\text{arcth}(\text{tg}\eta)}{k_0 L}. \quad (7.8)$$

7.2.3 Experimental Finding of Chirality Parameter Features

In order to investigate the dependence of the polarization properties of the dielectric bulk chiral structure on its “specific density” the experimental dependences of the rotation angle of the polarization plane $\theta(f)$ on the frequency of the electromagnetic wave $f = \omega/(2\pi)$ for four values of the structure thickness L (Fig. 7.3a) were analyzed [28]. Structure thickness L was varied from 10.5 to 12.6 mm by increasing the distance d between its layers from 1.5 to 1.8 mm. The “specific density” of the structure/metamaterial has been varied thereby. According to the experimental curves the frequency dependences of the chirality parameter real part $\kappa'(f)$ for several values of the structure thickness L (Fig. 7.3b) were calculated using the relation (7.8).

For the frequency dependence of the angle $\theta(f)$ for the structure thickness $L = 10.5$ mm (Fig. 7.3a, curve 1) near the frequency of 31.2 GHz the area of maximal dispersion of the $\theta = 90^\circ$ at the ellipticity angle $\eta = 20^\circ$ was defined. Near the frequency of 30 GHz the angle $\theta = 50^\circ$ at the $\eta = 2^\circ$. As can be seen, the

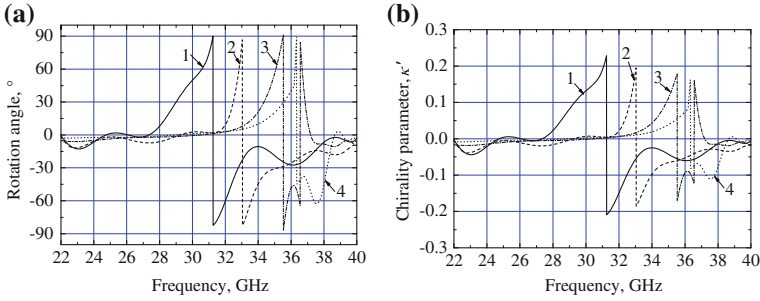


Fig. 7.3 Experimental frequency dependences: **a** $\theta(f)$ and **b** $\kappa'(f)$ for four values of the structure thickness L (l —10.5; 2—11.2; 3—11.9; 4—12.6 mm)

frequency dependence of the chirality parameter $\kappa'(f)$ is resonant at the same frequencies as for $\theta(f)$. The maximum for chirality parameter module reaches about 0.23. The dependence $\kappa'(f)$ is similar to the dependence $\theta(f)$ in accordance with formula (7.8).

Figure 7.4a clearly shows a monotonic increasing of the frequency f_{res} of the area of the maximal dispersion of the angle θ from 31.2 to 36.3 GHz with the structure “specific density” increasing. Such behavior can be assigned to existence of high-quality “magnetic” mode [8, 29], appeared in the given chiral medium. This “magnetic mode” has anomalous frequency dependence, i.e., when the distance between the layers of the chiral structure increases its frequency increases too. Such dependence is typical for media with negative dispersion. Note that in this bulk chiral structure, as well as structures in [8, 30] exists the “electric” mode, which has a conventional frequency dependence, i.e., when the distance between the layers of the chiral structure (the “specific density”) increases its frequency decreases.

Besides the decreasing of the maximum value of chirality parameter real part κ'_{res} from 0.23 to 0.16 (Fig. 7.4b) is registered at the same frequencies. The most probable reason for the decreasing of κ'_{res} is the exhausting of the structure with an increasing of the distance between its layers.

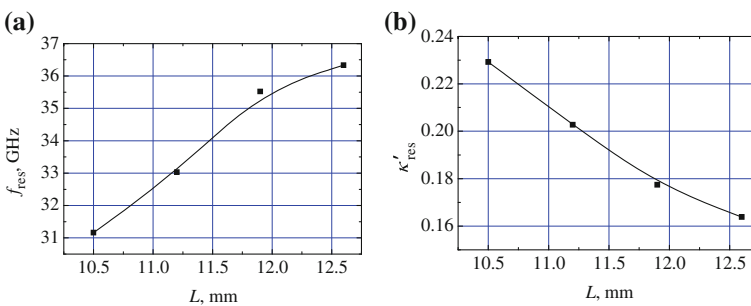


Fig. 7.4 Values of **a** $f_{\text{res}}(L)$ and **b** $\kappa'_{\text{res}}(L)$ for the “magnetic” mode

7.3 Faraday Effect Enhancement (FEE) in the Magnetoactive Bulk Metamaterial

7.3.1 The Experimental Technique

For the studying of the magnetoactive metamaterials with longitudinal magnetization another one experimental setup was design (Fig. 7.5). It is similar to the experimental setup described above, however, the structure and horns in it are located along the axis of the electromagnet that controlled by a computer. More detailed technique of this experiment is described in [15, 17].

The magnetoactive metamaterial being under investigation is designed as a single-layered structure, which consists of the planar chiral periodic structure placed on the ferrite (L14H) plane-parallel slab. The chiral structure is made of fiberglass, one side of which is covered with copper foil. The foil side of this structure is patterned with the periodic array whose square unit cell consists of the planar chiral rosette (see Fig. 7.2).

The polarization properties of the magnetoactive bulk metamaterial (Fig. 7.6), represents a multilayered structure. It consists from the set of single-layered magnetoactive structures described above.

7.3.2 Experimental. Polarization Rotation

Let consider some experimental results to demonstrate the influence of the magnetodependent elements involved into chiral media on its gyrotropy features under conditions of longitudinal magnetization:

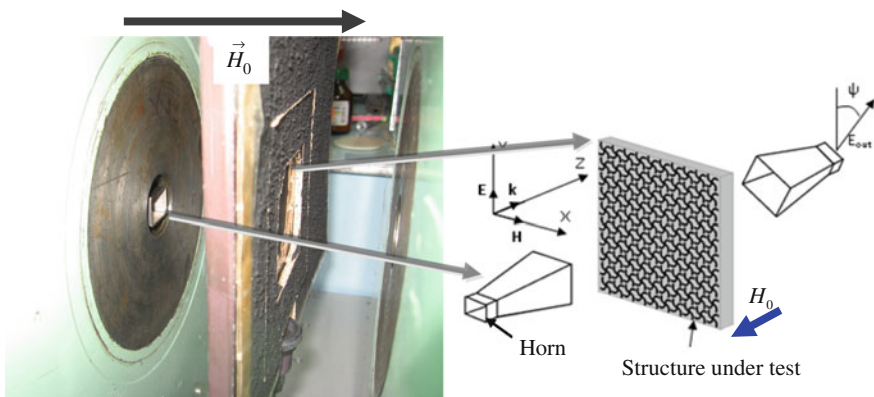


Fig. 7.5 The experimental setup for the study of magnetoactive structures with longitudinal magnetization

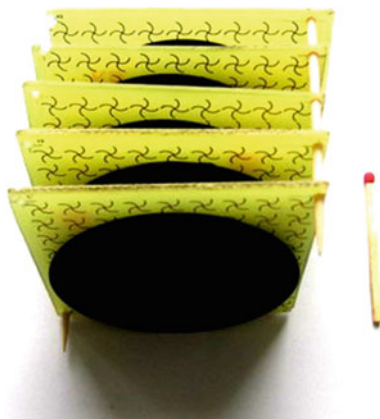


Fig. 7.6 The layered bulk magnetoactive metamaterial

- the polarization rotation angle θ of linearly polarized wave, propagating through a single ferrite slab (Fig. 7.7a);
- the polarization rotation angle θ of linearly polarized wave propagating through the magnetoactive bulk metamaterial consisting of planar chiral structure with period $d = 5$ mm loaded with a ferrite slab (Fig. 7.7b).

One can see that the surface plotted for the ferrite slab (Fig. 7.7a) is much smoother (colors variation is more weak) than that one for the one-layered magnetoactive metamaterial (Fig. 7.7b). Also, for the magnetoactive metamaterial, a monotonic growth of θ on the field strength takes place. Moreover, near the frequency of the metamaterial resonance dip ($f_r = 25.5\text{--}26.5$ GHz), this dependence acquires a pronounced resonant character (dashed line), and for $\theta \rightarrow \theta_r$ achieves significantly higher values than that one for the ferrite slab (up to $\theta_r \geq 45^\circ$).

It can be seen that the value θ_r (Fig. 7.7b) also depends on the magnetic field strength, and the maximum of θ_r is observed at $H_0 \approx 4800$ Oe (see arrow in

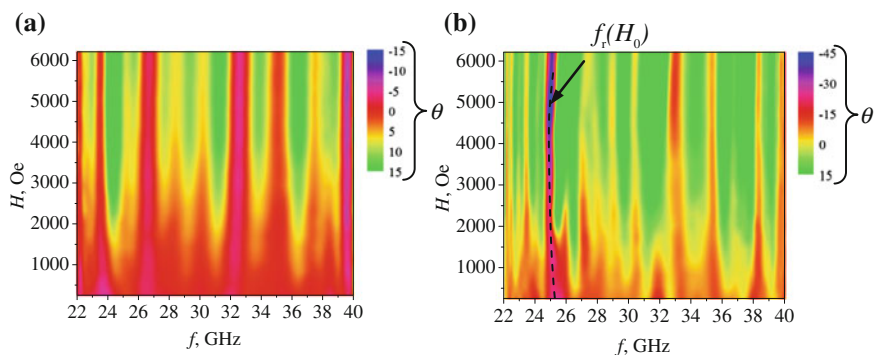


Fig. 7.7 Experimental dependencies of the polarization rotation angle $\theta(f, H_0)$ for: **a** the single ferrite slab; **b** the one-layered magnetoactive metamaterial

Fig. 7.8 The dependence of the rotation angle of the polarization plane on the static magnetic field for the layered bulk magnetoactive metamaterial

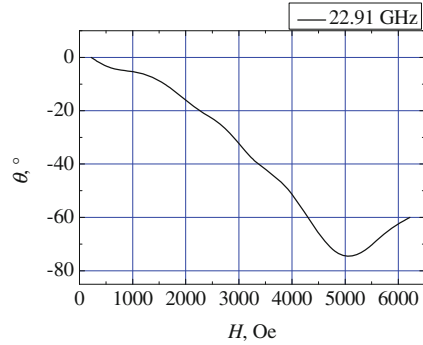


Fig. 7.7b). In this region the real part of permeability has extreme value, that explains the extreme in the dependency of $\theta_r(H_0)$.

The distinct feature of the bulk 1-layered magnetoactive chiral metamaterial is larger sensitivity of its polarization properties to the static magnetic field strength compared with single ferrite slab. This phenomenon can be explained by the fact that the resonant character of the magnetic permeability component of ferrite is superimposed on the resonant character of oscillations in the planar chiral structure.

Note that a similar situation, which was called as the amplification of the Faraday rotation has been detected by authors in the millimeter wave range earlier, but in more simple resonant structures (the two-mirror resonator [31]).

The similar measurements of the polarization characteristics for the layered bulk magnetoactive metamaterial (Fig. 7.6) were performed for the same values of the static magnetic field and microwave frequencies. At the frequency of 22.91 GHz at the static magnetic field of about 5000 Oe the rotation angle of the polarization plane reaches 75° (Fig. 7.8), that is sufficiently higher than for a single-layer magnetoactive chiral structure (Fig. 7.7b).

7.4 Faraday Effect Enhancement (FEE) in a Magnetoactive Bounded Photonic Crystal

7.4.1 The Experimental Technique

To realize the Faraday effect enhancement in the PC, that is limited by negative permittivity “boundary medium” described earlier experimental setup has been upgraded. The magentoactive element (ferrite disk) is placed between PC and the boundary medium (Fig. 7.9a). For the registration of the transmission coefficient of PCs in a given frequency range under the static magnetic field the technique [17] and the setup was used (Fig. 7.5). The electrodynamic cell (Fig. 7.9b) is a single-mode circular waveguide (with fundamental mode TE_{11}) contained the structure under research.

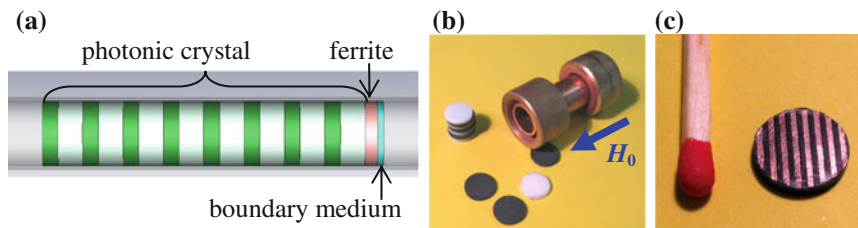


Fig. 7.9 **a** The model of investigated PC structure, loaded with magentoactive element and boundary medium; **b** The appearance of the electrodynamic cell for research in the cylindrical magnetophotonic structures; **c** the appearance of copper wire medium as the boundary of the photonic crystal

The investigated photonic crystal structures (Fig. 7.9b) consists of dielectric disks of different thicknesses and materials, so that the band gaps of such PC are located in the frequency range 22–40 GHz. As the boundary medium of PCs, the copper wire medium (Fig. 7.9c) and the copper thin film medium were used. The static magnetic field H_0 is directed along the axis of the cell.

7.4.2 Polarization Rotation in Magnetoactive Bounded Photonic Crystal. Experiment

Let consider the structures with the boundary medium as a thin metal film. Analysis of the transmission spectrum [17] of the unloaded PC (without boundary medium) and for the PC, loaded with ferrite slab and metal layer, shows that in the latter case, a surface state mode in the bandgap of PC (“surface peak” in Fig. 7.10) occurs. The peak has a common origin with the known Tamm peak [22, 32], so it will be also called as the Tamm peak.

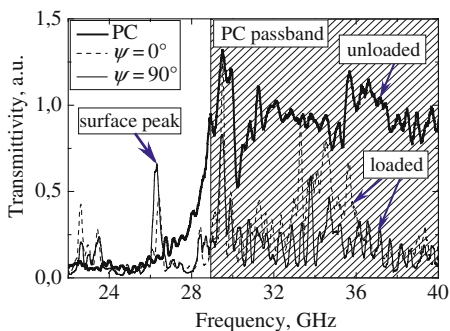


Fig. 7.10 The transmission spectrum of unloaded PC structure and PC structure loaded with ferrite slab and metal film for two different polarization angles of the incident wave

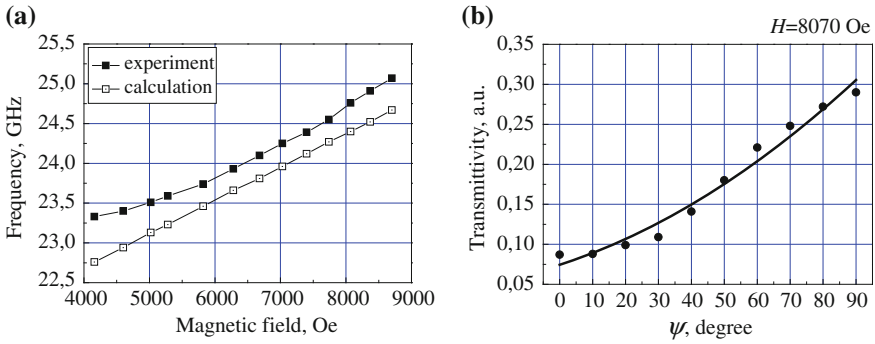


Fig. 7.11 **a** Tamm peak frequency versus: the static magnetic field; **b** the Tamm peak intensity versus the angle ψ

A detailed analysis allows to identify this peak as the peak associated with the excitation of TE_{11} mode, which is excited due Faraday effect in the ferrite layer. It can be seen (Fig. 7.10), when the angle between the polarization of the waveguide sections (transmitting and receiving) is $\psi = 90^\circ$, we can see more intense signal on the Tamm peak frequency in comparison with the case $\psi = 0^\circ$. Thus the Faraday effect enhancement takes place.

To check the nature of Tamm peak, we analyzed the dependence of its position on the static magnetic field, and the dependence of the peak intensity on the polarization angle (Fig. 7.11). It can be seen that if the peak associated with the Faraday effect, while increasing the magnetic field shifts in the higher frequency range. The numerical calculations [17] lead to the same conclusion. Really, in Fig. 7.11a typical experimental and calculated frequency-field dependences of the Tamm-peaks exhibit a similar behavior.

Polarization properties of the structure were studied experimentally by rotating the transmitting and receiving sections relatively to each other. Figure 7.11b shows the typical dependence of the surface state peak intensity on the angle ψ at some certain magnetic field $H = 8070$ Oe. It can be seen that with the increasing of the angle ψ the transmission coefficient is also increases. Its maximum is occurred at $\psi = 90^\circ$. This means that the polarization of the wave at the output of the structure is changed on 90° relative to the polarization at the input of the structure.

7.5 Conclusions

To conclude, let's list some outcomes of the research performed. Thus in the millimeter waveband:

1. Two experimental approaches for determining the effective constitutive parameters of the bulk chiral media are realized. The frequency dependence of

the real part of the chirality parameter of the bulk chiral metamaterial based on array of planar chiral structures is defined.

2. The ability to control the resonant frequency of the rotation angle of the polarization plane of electromagnetic wave by changing the “specific density” of the bulk metamaterial is demonstrated experimentally. The existence of left-handed “magnetic” mode is shown.
3. The transmission of electromagnetic waves through the multilayered and one-layered magnetoactive chiral metamaterial has been studied. The range of frequencies and magnetic field strength where the angle of polarization rotation appears essentially higher than that one related to a single ferrite slab (Faraday effect enhancement) is defined. The amplification of the polarization rotation for multilayered structure in comparison with one-layered structure is shown.
4. The surface state peak (the Tamm peak) was detected in the spectrum of the magnetoactive bounded photonic crystal. It was shown that the Tamm peak frequency depends on the external magnetic field.

Acknowledgments The authors thank Ruban V. P. for help in preparing of the investigating samples. The paper is supported partially by STCU grant #5714.

References

1. A. Serdyukov, I. Semchenko, S. Tretyakov, A. Sihvola, *Electromagnetics of Bi-anisotropic Materials: Theory and Applications* (Gordon and Breach Science Publishers, Amsterdam, 2001)
2. A. Sihvola, *Metamaterials in electromagnetics*. *Metamaterials* **1**(1), 2–11 (2007)
3. A.G. Gurevich, G.A. Melkov, *Magnetization Oscillations and Waves* (CRC Press, New York, 1996)
4. O.V. Ivanov, *Electromagnetic Wave Propagation in Anisotropic and Bianisotropic Layered Structures* (UISTU, Ulyanovsk, 2010). (in Russian)
5. O.V. Osipov, A.N. Volobuev, On the physical sense of material equations of a chiral medium. *Tech. Phys. Lett.* **35**(8), 753–755 (2009)
6. V.M. Agranovich, V.L. Ginzburg, *Spatial Dispersion in Crystalloptics and the Theory of Excitons* (Wiley-Interscience, London, 1966)
7. F.I. Fedorov, *Theory of Gyrotropy* (Nauka i Tekhnika, Minsk, 1976). (in Russian)
8. E. Plum, J. Zhou, J. Dong, V.A. Fedotov, T. Koschny, C.M. Soukoulis, N.I. Zheludev, Metamaterial with negative index due to chirality. *Phys. Rev. B.* **79**(3), 035407 (2009)
9. R. Zhao, L. Zhang, J. Zhou, Th Koschny, C.M. Soukoulis, Conjugated gammadion chiral metamaterial with uniaxial optical activity and negative refractive index. *Phys. Rev. B.* **83**(3), 035105 (2011)
10. S.L. Prosvirnin, V.A. Dmitriev, Electromagnetic wave diffraction by array of complex-shaped metal elements placed on ferromagnetic substrate. *Eur. Phys. J. Appl. Phys.* **49**(3), 33005 (2010)
11. V.A. Fedotov, P.L. Mladyonov, S.L. Prosvirnin, A.V. Rogacheva, Y. Chen, N.I. Zheludev, Asymmetric propagation of electromagnetic waves through a planar chiral structure. *Phys. Rev. Lett.* **97**(16), 167401 (2006)

12. L. Hecht, L.D. Barron, Linear polarization Raman optical activity. The importance of the non-resonant term in the Kramers-Heisenberg-Dirac dispersion formula under resonance conditions. *Chem. Phys. Lett.* **225**(4–6), 519–524 (1994)
13. L.R. Arnaut, L.E. Davis, On planar chiral structures, in *Progress in Electromagnetic Research Symposium PIERS 1995*, July, Seattle, p. 165 (1995)
14. S. Zouhdi, G.E. Couenon, A. Fourier-Lamer, Scattering from a periodic array of thin planar chiral structures—calculations and measurements. *IEEE Trans. Antennas Propagat.* **47**(6), 1061–1065 (1999)
15. S.Y. Polevoy, S.L. Prosvirnin, S.I. Tarapov, V.R. Tuz, Resonant features of planar Faraday metamaterial with high structural symmetry. *Eur. Phys. J. Appl. Phys.* **61**(3), 030501 (2013)
16. M. Inoue, R. Fujikawa, A. Baryshev, A. Khanikaev, P.B. Lim, H. Uchida, O.A. Aktsipetrov, T.V. Murzina, A.A. Fedyanin, A.B. Granovsky, Magnetophotonic crystals. *J. Phys. D Appl. Phys.* **39**(8), 151 (2006)
17. A.A. Girich, S.Y. Polevoy, S.I. Tarapov, A.M. Merzlikin, A.B. Granovsky, D.P. Belozorov, Experimental study of the Faraday effect in 1D-photonic crystal in millimeter waveband. *Solid State Phenom.* **190**, 365–368 (2012)
18. I.E. Tamm, O vozmozhnoi svyazi elektronov na poverkhnostiakh kristalla (in Russian). *Zh. Eksp. Teor. Fiz.* **3**(1), 34–35 (1933)
19. I.M. Lifshitz, S.I. Pekar, Tamm bounded states of electrons on the crystal surface and surface oscillations of lattice atoms (in Russian). *Usp. Fiz. Nauk.* **56**(8), 531–568 (1955)
20. S.V. Chernovtsev, S.I. Tarapov, D.P. Belozorov, Magnetically controllable 1D magnetophotonic crystal in millimetre wavelength band. *J. Phys. D Appl. Phys.* **40**(2), 295–299 (2007)
21. S.I. Tarapov, D.P. Belozorov, Microwaves in Dispersive Magnetic Composite Media (Review Article). *Low Temp. Phys.* **38**(7), 766–792 (2012)
22. A.P. Vinogradov, A.V. Dorofeenko, S.G. Erokhin, M. Inoue, A.A. Lisyansky, A.M. Merzlikin, A.B. Granovsky, Surface state peculiarities at one-dimensional photonic crystal interfaces. *Phys. Rev. B* **74**(4), 045128 (2006)
23. A.A. Bulgakov, A.A. Girich, M.K. Khodzitsky, O.V. Shramkova, S.I. Tarapov, Transmission of electromagnetic waves in a magnetic fine-stratified structure. *JOSA B* **26**(12), 156–160 (2009)
24. S.Y. Polevoy, S.L. Prosvirnin, S.I. Tarapov, Resonance properties of planar metamaterial, formed by array of gammadions on unmagnetized ferroelectric substrate. *Radiophys. Electron.* **4**(18), N1, 42–46 (2013) (in Russian)
25. R. Zhao, T. Koschny, C.M. Soukoulis, Chiral metamaterials: retrieval of the effective parameters with and without substrate. *Opt. Express* **18**(14), 14553–14567 (2010)
26. I.V. Lindell, A.H. Sihvola, S.A. Tretyakov, A.J. Viitanen, *Electromagnetic Waves in Chiral and Bi-Isotropic Media* (Artech House, Boston/London, 1994)
27. C. Menzel, C. Rockstuhl, T. Paul, F. Lederer, Retrieving effective parameters for quasiplanar chiral metamaterials. *Appl. Phys. Lett.* **93**(23), 233106 (2008)
28. S.Y. Polevoy, Experimental determination of constitutive parameters of the chiral media in the millimeter wavelength range. *Radiophys. Electron.* **4**(18), N4, 42–46 (2013) (in Russian)
29. S.Y. Polevoy, S.I. Tarapov, Frequency dispersion of the polarization properties of chiral structure in the millimeter waveband, in *The proceedings of the eighth international Kharkov symposium on physics and engineering of microwaves, millimeter and submillimeter waves MSMW 2013*, June 23–28, Kharkov, Ukraine, pp. 98–100 (2013)
30. J. Dong, J. Zhou, T. Koschny, C. Soukoulis, Bi-layer cross chiral structure with strong optical activity and negative refractive index. *Opt. Express* **17**(16), 14172–14179 (2009)
31. S.I. Tarapov, Y.P. Machekhin, A.S. Zamkovoy, *Magnetic Resonance for Optoelectronic Materials Investigation* (Collegium, Kharkov, 2008)
32. E. Yablonoitch, Inhibited spontaneous emission in solid-state physics and electronics. *Phys. Rev. Lett.* **58**(20), 2059–2062 (1987)